J|A|C|S ARTICLES

Published on Web 07/10/2009

Searching for Microporous, Strongly Basic Catalysts: Experimental and Calculated ^{29}Si NMR Spectra of Heavily Nitrogen-Doped Y Zeolites

Fulya Dogan,[†] Karl D. Hammond,[‡] Geoffrey A. Tompsett,[‡] Hua Huo,[†] W. Curtis Conner, Jr.,[‡] Scott M. Auerbach,[‡,§] and Clare P. Grey*,[†]

Department of Chemistry, State University of New York at Stony Brook, Stony Brook, New York 11794-3400, Department of Chemical Engineering, University of Massachusetts, Amherst, Massachusetts 01003-3110, and Department of Chemistry, University of Massachusetts, Amherst, Massachusetts 01003-9336

Received April 18, 2009; E-mail: cgrey@notes.cc.sunysb.edu

Abstract: Nitrogen substituted zeolites with high crystallinity and microporosity are obtained by nitrogen substitution for oxygen in zeolite Y. The substitution reaction is performed under ammonia flow by varying the temperature and reaction time. We examine the effect of aluminum content and charge-compensating cation ($H^+/Na^+/NH_4^+$) on the degree of nitrogen substitution and on the preference for substitution of Si−O−Al vs Si−O−Si linkages in the FAU zeolite structure. Silicon-29 magic angle spinning (MAS) nuclear magnetic resonance (NMR) and ^{1}H/^{29}Si cross-polarization MAS NMR spectroscopy have been used to probe the different local environments of the nitrogen-substituted zeolites. Experimental data are compared to simulated NMR spectra obtained by constructing a compendium (>100) of zeolite clusters with and without nitrogen, and by performing quantum calculations of chemical shifts for the NMR-active nuclei in each cluster. The simulated NMR spectra, which assume peak intensities predicted by statistical analysis, agree remarkably well with the experimental data. The results show that high levels of nitrogen substitution can be achieved while maintaining porosity, particularly for NaY and low-aluminum HY materials, without significant loss in crystallinity. Experiments performed at lower temperatures (750−800 °C) show a preference for substitution at Si−OH−Al sites. No preference is seen for reactions performed at higher temperatures and longer reaction times (e.g., 850 °C and 48 h).

1. Introduction

Zeolites and other microporous silicates are widely used as acidic catalysts for size and shape selective catalytic reactions.[1−3] Much effort has been expended to identify microporous materials that can replace liquid basic catalysts, since microporous basic catalysts are noncorrosive, easily separated from the reaction mixture, and readily regenerated after the reaction.[4−6] Furthermore, the high surface area and shape selectivity of such materials[7−10] can be used to tune selectivities in base-catalyzed reactions. Such reactions are particularly important in light of recent interest in biomass conversion to produce fuels from renewable feedstocks.[11]

Basic zeolitic catalysts can be prepared by various methods such as ion-exchange with alkali metal cations,[8] impregnation with alkali metal ions/basic salts,[5] and grafting of organic bases onto the pore walls.[5] The resulting materials often suffer from instability and/or pore blockage, because none of these approaches place basic sites directly into the zeolite framework. In contrast, zeolitic materials have been made with some of the bridging oxygen atoms in Si−O−Si and/or Si−O−Al linkages replaced by CH_2 groups[12] or by NH groups,[13] in a process named nitridation. This is achieved by treating the material with amines such as ammonia at high temperatures. As a result, the base strength of the framework increases[14,15] due to the lower electronegativity of nitrogen with respect to oxygen, as con-

[†] State University of New York at Stony Brook.
[‡] Department of Chemical Engineering, University of Massachusetts.
[§] Department of Chemistry, University of Massachusetts.

(1) Auerbach, S. M., Carrado, K. A., Dutta, P. K., Eds. *Handbook of Zeolite Science and Technology*; Marcel-Dekker: New York, 2003.
(2) Weitkamp, J. *Solid State Ionics* **2000**, *131*, 175–188.
(3) Haw, J. F. *Phys. Chem. Chem. Phys.* **2002**, *4*, 5431–5441.
(4) Wan, K.; Liu, Q.; Zhang, C.; Wang, J. *Bull. Chem. Soc. Jpn.* **2004**, *77*, 1409–1414.
(5) Weitkamp, J.; Hunger, M.; Rymsa, U. *Microporous Mesoporous Mater.* **2001**, *48*, 255–270.
(6) Barthomeuf, D. *Microporous Mesoporous Mater.* **2003**, *66*, 1–14.
(7) Narasimharao, K.; Hartmann, M.; Thiel, H. H.; Ernst, S. *Microporous Mesoporous Mater.* **2006**, *90*, 377–383.
(8) Zhang, X.; Lai, E. S. M.; Aranda, R. M.; Yeung, K. L. *Appl. Catal. A Gen.* **2004**, *261*, 109–118.
(9) Ernst, S.; Hartmann, M.; Sauerbeck, S.; Bongers, T. *Appl. Catal. A Gen.* **2000**, *200*, 117–123.
(10) Zhang, C.-M.; Xu, Z.; Wan, K.-S.; Liu, Q. *Appl. Catal. A Gen.* **2004**, *258*, 55–61.
(11) Suppes, G. J.; Dasari, M. A.; Doskocil, E. J.; Mankidy, P. J.; Goff, M. J. *Appl. Catal. A Gen.* **2004**, *257*, 213–223.
(12) Yamamoto, K.; Sakata, Y.; Nohara, Y.; Takahashi, Y.; Tatsumi, T. *Science* **2003**, *300*, 470–472.
(13) Kerr, G. T.; Shipman, G. F. *J. Phys. Chem.* **1968**, *72*, 3071–3072.
(14) Han, A.-J.; He, H.-Y.; Guo, J.; Yu, H.; Huang, Y.-F.; Long, Y.-C. *Microporous Mesoporous Mater.* **2005**, *79*, 177–184.
(15) Xiong, J. M.; Ding, Y. J.; Zhu, H. J.; Yan, L.; Liu, X. M.; Lin, L. W. *J. Phys. Chem. B* **2003**, *107*, 1366–1369.

10.1021/ja9031133 CCC: $40.75

firmed by recent density functional theory (DFT) calculations.[16−18] Although interest in such materials has intensified since 2000,[9] microscopic understanding of active sites and residual framework structure is often indirect at best and sometimes nonexistent. In this paper, we present synthesis, detailed characterization, and quantum-simulated NMR spectra pinpointing the nature of both framework sites and zeolite structure in heavily nitrogen-doped zeolite Y.

Substitution of framework oxygen with nitrogen has been performed on several different oxides such as amorphous silica, aluminophosphates, and mesoporous silicon oxides such as SBA-15 and MCM-41.[19−24] Crystalline zeolites are more difficult to nitride as they contain fewer silanol groups as defect sites and it has been claimed by some authors that the nitrogen substitution reaction starts from these defect sites.[15,23] Furthermore, ammonia treatment of zeolites at high temperatures can result in loss of crystallinity. Despite these difficulties, we establish conclusively the formation of zeolites with framework nitrogen and minimal loss of zeolite structure. In particular, we present the synthesis and detailed characterization of nitrided zeolite Y with high levels of nitrogen substitution, high crystallinity, and high porosity. We establish this by combining X-ray, NMR, and density functional theory (DFT) calculations to determine the signatures of various nitrogen environments. We have chosen to work with zeolite Y for several reasons. Zeolite Y exhibits the FAU type of structure, whose large pores allow access by relatively large molecules. Its highly symmetric structure means that it is only necessary to model one crystallographic site (T site) for every different silicon environment. This limits the number of calculations that must be performed to model nitrogen substitutions in the structure.

The structural properties of nitrided zeolites and mesoporous materials have previously been investigated by various analytical methods. Powder X-ray diffraction has been used to study the changes in the crystallinity of the material after the reaction;[9,14] Fourier transform infrared (FT-IR) and FT-Raman spectroscopy methods have been used to characterize the nitrogen-substituted surface groups and unreacted defect silanol groups;[14,19] and elemental analysis has been employed to determine nitrogen content.[10,19] However, few studies have focused on characterizing these materials by ^{29}Si solid state Magic Angle Spinning (MAS) Nuclear Magnetic Resonance (NMR) spectroscopy,[4,10,19,20] and no experimental NMR study has yet to (a) demonstrate high nitridation levels and (b) consider how aluminum in the framework may influence the NMR spectrum of the nitrided zeolite.

Silicon-29 MAS NMR spectroscopy is a very sensitive tool with which to study local environments for silicon in the zeolite framework. In general, the chemical shifts become less negative with increasing Si−O bond length, decreasing T−O−T bond angle, or with decreasing the electronegativity of the surrounding atom.[25] For example, substitution of aluminum for silicon in the framework causes a shift of approximately 5 ppm per aluminum atom. Previous ^{29}Si NMR experimental studies on nitrided zeolites and mesoporous materials[4,10,19,26] and our recent quantum mechanical calculations[24] have shown that substitution of nitrogen for oxygen in the zeolite framework results in an even larger shift to less negative values of chemical shift, providing a sensitive method to study the degree of nitridation. Zhang et al.,[10] in one of the very few ^{29}Si NMR studies of a nitrided zeolite, observed only one new site in ZSM-5 with Si/Al = 50, with a single extra resonance near −90 ppm, (even though they reported a nitridation level of 16% by weight) which they assigned to an $SiNO_3$ environment. A larger range of silicon environments was observed in another study of silicon oxynitrides, at −90 to −48 ppm, which were assigned to $SiO_{4-x}N_x$ environments with x = 1, 2, 3, and 4, respectively.[19] The assignment of resonances in both silicon oxynitrides and zeolites is, however, complicated by the presence of possible terminal amine/hydroxyl groups and the effect of framework aluminum on the nitrogen shifts. We address this latter issue by integrating experiment and theory of ^{29}Si NMR, yielding a detailed picture of the interplay between aluminum and nitrogen substitution.

Quantum chemistry is used here to calculate the energies and ^{29}Si chemical shifts of different nitrogen environments in the zeolite framework, allowing us to compute nitrogen doping levels as controlled by temperature, reaction time, and aluminum content in the zeolites studied. To accomplish this, we have performed rigorous analyses of both ^{29}Si NMR peak positions *and* peak intensities, essentially yielding "quantum simulations" of the NMR spectra. We note that most previous studies reporting quantum modeling of zeolite NMR spectra provide only tables of chemical shifts.[27] In contrast, we model the spectra by assuming Lorentzian line shapes with intensities predicted by statistical analysis of nitrogen and aluminum siting frequencies in the materials studied. To parametrize the spectra, we have constructed a compendium (>100) of zeolite clusters with and without nitrogen, and have performed quantum calculations of chemical shifts for the NMR-active nuclei in each cluster. The resulting simulated NMR spectra agree remarkably well with experiment.[24]

This paper presents a detailed microscopic picture showing the effects of Si/Al ratio, H^+ vs Na^+ extra-framework cations, and temperature on reactivity, degree of nitrogen substitution, and framework stability. We show that the highest levels of nitridation and crystallinity are obtained by using zeolites with low aluminum content. We first present X-ray diffraction, nitrogen content analysis, and adsorption data, followed by a comparison of the calculated chemical shifts for a wide range of different nitrided silicon environments. We then describe experimentally observed single pulse (SP) and cross-polarization (CP) ^{29}Si MAS NMR spectra. The calculated ^{29}Si chemical shifts are then used to simulate the experimental spectra and explore the preferential substitution of NH/NH_2 in Si−O−Al vs

(16) Astala, R.; Auerbach, S. M. *J. Am. Chem. Soc.* **2004**, *126*, 1843–1848.
(17) Lesthaeghe, D.; Van Speybroeck, V.; Waroquier, M. *J. Am. Chem. Soc.* **2004**, *126*, 9162–9163.
(18) Lesthaeghe, D.; Van Speybroeck, V.; Marin, G. B.; Waroquier, M. *J. Phys. Chem. B* **2005**, *109*, 7952–7960.
(19) Zhang, C.; Liu, Q.; Xu, Z. *J. Non-Cryst. Solids* **2005**, *351*, 1377–1382.
(20) El Haskouri, J.; Cabrera, S.; Sapiña, F.; Latorre, J.; Guillem, C.; Beltrán-Porter, A.; Beltrán-Porter, D.; Marcos, M. D.; Amorós, P. *Adv. Mater.* **2001**, *13*, 192–195.
(21) Wan, K.; Liu, Q.; Zhang, C. *Chem. Lett.* **2003**, *32*, 362–363.
(22) Kapoor, M. P.; Inagaki, S. *Chem. Lett.* **2003**, *32*, 94–95.
(23) Chino, N.; Okubo, T. *Microporous Mesoporous Mater.* **2005**, *87*, 15–22.
(24) Hammond, K. D.; Dogan, F.; Tompsett, G. A.; Agarwal, V.; Conner, W. C.; Grey, C. P.; Auerbach, S. M. *J. Am. Chem. Soc.* **2008**, *130*, 14912–14913.
(25) Mackenzie, K. J. D.; Smith, M. E. *Multinuclear Solid-State NMR of Inorganic Materials*; Pergamon Material Series; Pergamon: Oxford, 2002; Vol. 6.
(26) Xia, Y.; Mokaya, R. *J. Phys. Chem. C* **2008**, *112*, 1455–1462.
(27) Bull, L. M.; Bussemer, B.; Anupld, T.; Reinhold, A.; Samoson, A.; Sauer, J.; Cheetham, A. K.; Dupree, R. *J. Am. Chem. Soc.* **2000**, *122*, 4948–4958.

Si−O−Si positions. We find high levels of nitrogen substitution can be achieved while maintaining porosity, particularly for NaY and low-aluminum HY materials, without significant loss in crystallinity. Experiments performed at lower temperatures (750−800 °C) show a preference for substitution at Si−OH−Al sites. No preference is seen for reactions performed at higher temperatures and longer reaction times (e.g., 850 °C and 48 h).

2. Experimental Section

2.1. Synthesis. Commercial HY, Si/Al = 15 (CBV 720, Lot #72004N00868); NH_4Y, Si/Al = 2.55 (CBV 300, Lot #300001021451); NaY, Si/Al = 2.55 (CBV 100, Lot #100031042531); and HY, Si/Al = 2.55 (CBV 400, Lot #400054002618) from Zeolyst (Valley Forge, PA) were used as starting materials. The Si/Al values quoted here are provided by the manufacturer, and represent the overall Si/Al ratio, not necessarily the Si/Al ratio of the framework. Both dehydration and nitridation were accomplished in an alumina boat which was inserted into a quartz tube furnace with dimensions of 3.8 cm diameter and 72 cm in length. Dehydration of the samples prior to the nitridation was conducted under nitrogen flow. The temperature was slowly ramped to 110 at 0.1 °C/min, held at that temperature for 2 h, then slowly ramped to 400 at 0.5 °C/min, and held at that temperature for 10 h. Following this dehydration step, several samples were prepared by heating the samples in flowing nitrogen to 550 °C, then initiating a high ammonia flow rate of approximately 2000 cm^3/min. The temperature was then raised to the final nitridation temperature. Subsequently, the samples were cooled down to room temperature under nitrogen flow and stored in a nitrogen glovebox until needed for the characterization experiments. Since the temperatures quoted correspond to those measured with a thermocouple outside the quartz tube, we also determined the temperature near the center of the tube using the same flow rates and only a 5 °C difference between the measured and actual sample temperatures was found in our experimental setup.

The samples for the characterization experiments were all prepared in a glovebox with dry nitrogen atmosphere. The following nomenclature is used to label the samples: The first label "Nit" indicates that zeolites are nitrided. The type of the zeolite (e.g., HY, NaY) and Si/Al ratio is then given, which is followed by the nitridation temperature in °C and the treatment duration in hours. For example, the label "Nit-HY-15−850−24" refers to a nitrided, HY zeolite with Si/Al = 15, treated at 850 °C for 24 h.

2.2. Characterization. Powder X-ray diffraction patterns were collected on a Rigaku diffractometer using Cr K-α radiation (wavelength 0.229 nm). The 2θ values were converted with respect to Cu K-α (wavelength 0.154 nm) for ease of comparison. Elemental analyses of the nitrided samples for nitrogen content were carried out by Galbraith Laboratories Inc. (Knoxville, TN), by a combustion reaction using a PerkinElmer 240 Elemental Analyzer (PerkinElmer; Waltham, MA). The Kjeldahl method,[28] performed at Galbraith Laboratories, was also used to check the accuracy of different methods for nitrogen elemental analysis. Energy dispersive X-ray spectroscopy (EDX) measurements were carried out on a LEO-1550 field emission scanning electron microscope (SEM) operating at an accelerating voltage of 20 kV. Adsorption analyses were performed by using a Micromeritics ASAP 2010 surface analyzer (Micromeridics Corp.; Norcross, GA). Surface areas were estimated using the BET equation, and micropore volumes were determined using the *t*-plot method[29] using the universal thickness model of deBoer.[30]

The ^{29}Si MAS NMR analysis was performed on a Varian 360 MHz spectrometer with a 4 mm probe using 14 and 8 kHz MAS for the single pulse (SP) and ^{1}H−^{29}Si CP experiments, respectively. The ^{29}Si and ^{1}H 90° pulses were 2.4 and 4.5 μs, respectively. The RF field strengths for ^{1}H−^{29}Si CP experiments are ∼42 and ∼100 kHz for ^{29}Si and ^{1}H, respectively. Contact times of 0.1 to 10 ms were used in the CP experiments. Pulse delays of 30 s were used for the ^{29}Si MAS NMR experiments. The spin−lattice relaxation times (T_1) measured on select samples (Nit-HY-15−850−24 and Nit-NaY-2.55−850−24) were approximately 15 s for each silicon site (i.e., no differences in T_1 values were determined for the different environments).Thus, as pulse delays of 30 s was considered sufficient to ensure qualitatively reliable intensities. The ^{29}Si chemical shifts were referenced to tetramethylsilane (TMS) at 0 ppm. All the dehydrated/nitrided samples were packed into NMR rotors under dried nitrogen atmosphere in a glovebox.

The Si/Al ratios of the pristine materials were calculated from the SP ^{29}Si NMR data, according to "Loewenstein's rule"[31] (which stipulates that no Al−O−Al linkages can occur in the zeolite framework), with the following equation:[32]

$$\frac{\mathrm{Si}}{\mathrm{Al}} = \sum_{x=0}^{4} I_{\mathrm{Si(OAl)}_x} / 0.25 \sum_{x=0}^{4} x I_{\mathrm{Si(OAl)}_x} \qquad (1)$$

3. Theoretical

3.1. Quantum Mechanical Calculations. The theory of chemical shifts as it pertains to electronic structure calculations is nicely summarized by Gauss.[33] While implementations of NMR calculations using DFT with periodic boundary conditions exist,[34−36] these methods are impractical for our present use due to the large size of the FAU unit cell and our need to calculate multiple defect structures. Instead, we studied a small fragment of the FAU framework containing 14 tetrahedral (Si, Al) atoms. This cluster contains two central tetrahedral atoms and one oxygen atom that are three or more coordination shells away from the terminating hydrogen atoms. Bussemer and coworkers[37] found that this is sufficient to converge chemical shielding with respect to system size. We performed a series of calculations on a cluster with 23 T sites to confirm this; in such a cluster, the central silicon atom is *five* layers from the terminating hydrogen atoms, and the cluster contains a larger zeolite fragment. The resulting chemical shifts are within 1 ppm of the chemical shifts of the 14T clusters. Our 14 T-site cluster was centered around the O^{IV} site, following the standard numbering.[38] The cluster was terminated with hydroxide groups,

(28) ASTM Standard D3590−02, "Standard Test Methods for Total Kjeldahl Nitrogen in Water," ASTM International, West Conshohocken, PA, 2006; DOI: 10.1520/ D3590−02R06, http://www.astm.org/.

(29) Sing, K. S. W. *Chem. Ind.* **1967**, 829–830.
(30) de Boer, J. H.; Lippens, B. C.; Linsen, B. G.; Broekhoff, J. C. P.; van den Heuvel, A.; Osinga, T. J. *J. Colloid Interface Sci.* **1966**, *21*, 405–414.
(31) Loewenstein, W. *Am. Mineral.* **1954**, *39*, 92–96.
(32) Fyfe, C. A.; Feng, Y.; Grondey, H.; Kokotailo, G. T.; Gies, H. *Chem. Rev.* **1991**, *91*, 1525–1543.
(33) Gauss, J. In *Modern Methods and Algorithms of Quantum Chemistry*, 2nd ed.; Grotendorst, J., Ed.; John von Neumann Institut für Computing: 2000; Vol. 3, pp 541−592.
(34) Mauri, F.; Pfrommer, B. G.; Louie, S. G. *Phys. Rev. Lett.* **1996**, *77*, 5300–5303.
(35) Gregor, T.; Mauir, F.; Car, R. *J. Chem. Phys.* **1999**, *111*, 1815–1822.
(36) Yates, J. R.; Pickard, C. J.; Payne, M. C. *J. Chem. Phys.* **2003**, *118*, 5746–5753.
(37) Bussemer, B.; Schröder, K.-P.; Sauer, J. *Solid State Nucl. Magn. Reson.* **1997**, *9*, 155–164.
(38) Smith, J. V. In *Molecular Sieve Zeolites−1*; Flanigen, E. M., Sand, L. B., Eds.; American Chemical Society: Washington, D.C., 1971; Vol. 101, pp 171−200.

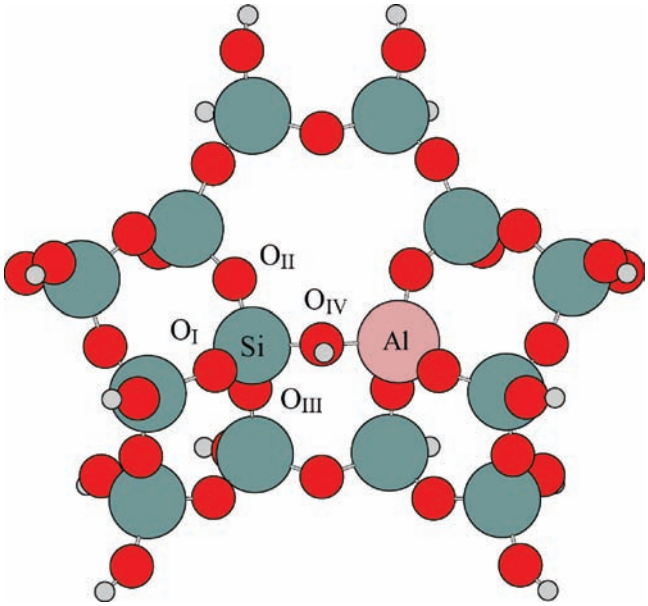

Figure 1. Zeolite cluster used in our calculations. Colors: gray, Si; brown, Al; red, O; white, H.

the hydrogen atoms of which were placed along the cleaved Si−O bond at approximately 0.86 Å from the oxygen. All terminal OH groups and any silicon atoms bound to two or more OH groups were fixed at their crystallographic coordinates during geometry optimization; this is necessary to ensure the final geometry is representative of FAU zeolite. A version of this cluster in which one silicon atom has been replaced by aluminum (with the compensating hydrogen atom) is shown in Figure 1. Hydrogen atoms were placed on the nitrogen or oxygen atom nearest the central silicon atom to avoid edge effects. This creates some other problems related to the fact that several protons are crowded near one tetrahedral site, which is discussed in section 4. Sodium ions were placed near positions SI, SI′, SII, and/or SIII in each cluster, and they were then allowed to relax. This is a crude approximation, as the real material would show a distribution of different cation arrangements. However, the change in the chemical shift when sodium ions are absent entirely (instead, the entire cluster has a negative change) is very small, indicating the effects of ion placement are less significant than other sources of error in the calculation. The placement of four Na^+ about the $Si(OAl)_4$ environment will be associated with the largest numbers of combinations. Hence the data reported in Table 3 is for the bare (charged) cluster.

Shielding tensors were computed using the method of gauge-including atomic orbitals (GIAO),[39,40] which has been demonstrated to improve the convergence of the calculated values with respect to basis set, when compared to other methods.[33,41] The calculations were performed using DFT with the B3LYP hybrid exchange-correlation functional[42−46] as implemented in Gaussian.[47] The geometry of each cluster was optimized using the 6-311G(*d,p*) basis set;[48,49] chemical shieldings were calculated using the (larger) cc-pVTZ basis set.[50−55]

All reported chemical shifts in this article are presented in parts per million from liquid tetramethylsilane (TMS), the standard reference compound for ^{29}Si NMR.[56] Gaseous silane (SiH_4) was employed as a secondary reference for the calculations, and the chemical shift (δ) is given by

$$\delta = \frac{\sigma_{\mathrm{ref}} - \sigma}{1 - \sigma_{\mathrm{ref}}} + \delta_{\mathrm{ref}} \qquad (2)$$

Silane has a chemical shift of $\delta_{\mathrm{ref}} = -104.34$ ppm from liquid TMS in the limit of zero pressure.[57] Choosing a different reference nucleus does *not* change the relative spacing of peaks in the NMR spectrum, only their absolute positions.

3.2. Spectral Generation. The outputs from a chemical shift calculation are the eigenvalues of the chemical shielding tensor. Interpreting these numbers in the form of a spectrum requires a model for line shapes, peak heights and peak widths (i.e., so-called integrals). Since ^{29}Si is a spin-1/2 nucleus, the line shape, L, for a single chemical environment can be described by a Lorentzian line shape:

$$L_i(\delta|g,\delta_i) = \frac{1}{\pi}\frac{g}{(\delta - \delta_i)^2 + g^2} \qquad (3)$$

The value of g is the half-width at half-maximum of the Lorentzian, which is determined by the spin−spin relaxation time, T_2, caused, for example, by residual interactions that are not completely removed by MAS (e.g., homonuclear dipolar coupling). In ^{29}Si MAS NMR, homonuclear coupling is negligible, and line broadening due to T_2 effects are much smaller than the *apparent* broadening (T_2*), which will also reflect the distribution of local environments; we model this broadening in our simulations.

The spectrum $S(\delta)$ is generated by multiplying each line shape by the fraction of silicon atoms in the zeolite that have that environment and summing over all environments: $S(\delta) = \sum_i I_i L_i(\delta|g,\delta_i)$, where I_i is the integral (fraction of silicon atoms) associated with line shape i. The value of g is a fitting parameter unique to each spectral feature in the system. With values of $\{\delta_i\}$ given by the electronic structure calculations (section 4.3.1), the only missing parameters are the intensities $\{I_i\}$.

We generated the integral of each peak (I_i) in the NMR spectrum by assuming a quasi-random distribution with various

(39) Ditchfield, R. *Mol. Phys.* **1974**, *27*, 789–807.
(40) Wolinski, K.; Hinton, J. F.; Pulay, P. *J. Am. Chem. Soc.* **1990**, *112*, 8251–8260.
(41) Cheeseman, J. R.; Trucks, G. W.; Keith, T. A.; Frisch, M. J. *J. Chem. Phys.* **1996**, *104*, 5497–5509.
(42) Becke, A. D. *Phys. Rev. A* **1988**, *38*, 3098–3100.
(43) Becke, A. D. *J. Chem. Phys.* **1993**, *98*, 5648–5652.
(44) Lee, C.; Yang, W.; Parr, R. G. *Phys. Rev. B* **1988**, *37*, 785–789.
(45) Vosko, S. H.; Wilk, L.; Nusair, M. *Can. J. Phys.* **1980**, *58*, 1200–1211.
(46) Stephens, P. J.; Devlin, F. J.; Chabalowski, C. F.; Frisch, M. J. *J. Phys. Chem.* **1994**, *98*, 11623–11627.
(47) Frisch, M. J.; et al. *GAUSSIAN Development Version*, Revision E.X2; Gaussian, Inc.: Wallingford, CT, 2004.
(48) McLean, A. D.; Chandler, G. S. *J. Chem. Phys.* **1980**, *72*, 5639–5648.
(49) Krishnan, R.; Binkley, J. S.; Seeger, R.; Pople, J. A. *J. Chem. Phys.* **1980**, *72*, 650–654.
(50) Dunning, T. H. *J. Chem. Phys.* **1989**, *90*, 1007–1023.
(51) Kendall, R. A.; Dunning, T. H.; Harrison, R. J. *J. Chem. Phys.* **1992**, *96*, 6796–6806.
(52) Woon, D. E.; Dunning, T. H. *J. Chem. Phys.* **1993**, *98*, 1358–1371.
(53) Peterson, K. A.; Woon, D. E.; Dunning, T. H. *J. Chem. Phys.* **1994**, *100*, 7410–7415.
(54) Davidson, E. R. *Chem. Phys. Lett.* **1996**, *260*, 514–518.
(55) EMSL Basis Set Exchange. [Online]. Pacific Northwest National Laboratory. https://bse.pnl.gov/bse/portal/.
(56) Harris, R. K.; Becker, E. D.; Cabral de Menezes, S. M.; Goodfellow, R.; Granger, P. *Pure Appl. Chem.* **2001**, *73*, 1795–1818.
(57) Makulski, W.; Jackowski, K.; Antušek, A.; Jaszuński, M. *J. Phys. Chem. A* **2006**, *110*, 11462–11466.

assumptions. The major differences in the chemical shifts of silicon atoms are due to second-neighbor aluminum atoms, associated cations, and the presence of nitrogen (for substituted materials). Loewenstein's rule[31] implies that all aluminum atoms are shared between exactly four silicon atoms, so the silicon NMR spectrum of the entire zeolite can be approximated as the sum over all possible combinations of nitrogen and oxygen as nearest neighbors and all possible combinations of silicon and aluminum as second-nearest neighbors, weighted according to their distribution. For the untreated zeolites, this distribution is the probability of finding x aluminum atoms near a central silicon atom, where $x \in \{0, 1, 2, 3, 4\}$. Vega[58] generated a model for the aluminum distribution that takes Loewenstein's rule and the resulting correlations between opposite corners of four-membered rings into account. We use his formulas for the intensities I_0-I_4 as a function of aluminum fraction herein, denoted p_x in the equations that follow.

The fractions of silicon in each environment for a *substituted* zeolite were calculated using the following assumptions. First, the distribution of aluminum near each silicon atom is given by the same distribution as that for the untreated material (denoted p_x). Second, the probability of nitrogen substituting near a particular silicon atom is independent of the number of nitrogen atoms already bound to that silicon atom. This assumption is based on the relatively small differences between the energies of two single-substitutions compared to one double-substitution (see Table 2). Our third assumption is actually a choice between several assumptions. One logical assumption is that substitutions occur at acid sites (due to their lower energy, discussed in section 4.3.1) unless all such sites have already been substituted. A second assumption is that since there are more Si−O−Si sites than acid sites (at least in low aluminum materials), substitution at these sites is preferred. A third alternative is that there is no preference between these, and substitution is equally likely at any site. We compare the results of each of these assumptions for each material in section 4.3.1.

The nitrogen distribution using these assumptions can be derived in the following way. We assume a fixed fraction, ζ, of the total oxygen atoms in the framework are substituted with nitrogen. This parameter is adjustable and represents the fractional yield of nitridation. The number of nitrogen atoms per repeating unit, n, is simply $n = 384\ \zeta$, since the FAU unit cell contains 384 oxygen atoms. We handle surface atoms by assuming a certain fraction of the silicon atoms, f, are "on the surface" (i.e., bound to one surface hydroxyl group). Let the number of silicons per repeating unit be s. The number of *surface* nitrogens (N_S) per surface silicon (Si_S) is $(N_S)/(Si_S) = \min(1, n/fs)$, and the number of nitrogen atoms in the framework (N_F) per framework silicon (Si_F) is

$$\frac{N_F}{Si_F} = \frac{n - sf\dfrac{N_S}{Si_S}}{s(1-f)} = \frac{n - sf\min\left(1, \dfrac{n}{fs}\right)}{s(1-f)} \tag{4}$$

If we assume Brønsted acid sites fill first (call this case a), the probability of a "Si−OH−Al" site being substituted with nitrogen is N_F/Si_F divided by the number of acid sites per framework silicon. If we call this probability a_{Al}, and the probability of a silicon atom being second-neighbor to x aluminum atoms p_x, then

$$a_{Al} = \min\left(1, \frac{N_F/Si_F}{\frac{1}{4}(p_1 + 2p_2 + 3p_3 + 4p_4)}\right) \tag{5a}$$

The factor of 1/4 in the denominator of eq 5a is due to the fact that the hydrogen atoms of the Brønsted acid sites are shared, on the average, between four different silicon atoms. If surface sites are absent, the denominator is equal to the Al/Si ratio. We note that this factor of 4 was missing in our earlier communication,[24] resulting in an overestimate of the substitution ratios (ζ). If $a_{Al} > 1$, it means all acid sites have been substituted, and therefore some Si−NH−Si sites must form. The probability of forming Si−NH−Si sites, a_{Si}, is

$$a_{Si} = \max\left(0, \frac{N_F/Si_F - \frac{1}{4}(p_1 + 2p_2 + 3p_3 + 4p_4)}{2p_0 + \frac{3}{2}p_1 + p_2 + \frac{1}{2}p_3}\right) \tag{5b}$$

The probability of a silicon near x aluminum atoms and with $y + z$ nitrogen atoms (y atoms between silicon and aluminum, z between two silicon atoms) is, in our model,

$$I_{xyz} = p_x a_{Al}^y (1 - a_{Al})^{x-y} \binom{x}{y} a_{Si}^z (1 - a_{Si})^{4-x-z} \binom{4-x}{z} \tag{6}$$

Note that $0^0 = 1$ in this model, since the proper limit is of the form $\lim_{\xi \to 0} \xi^0 = 1$. The probability given by eq 6 is equal to the integral of the NMR peak.

In the case where there is no bias toward either siliceous sites *or* acid sites (case b), eqs 5a and 5b become

$$b_{Al} = b_{Si} = \min\left(1, \frac{N_F/Si_F}{\frac{1}{4}(p_1 + 2p_2 + 3p_3 + 4p_4) + 2p_0 + \frac{3}{2}p_1 + p_2 + \frac{1}{2}p_3}\right) \tag{7}$$

and all instances of a in eq 6 are replaced by b.

In the case where siliceous sites [$Si(OSi)_4$] fill first (call this case c), eqs 5a and 5b become

$$c_{Al} = \max\left(0, \frac{N_F/Si_F - \left(2p_0 + \frac{3}{2}p_1 + p_2 + \frac{1}{2}p_3\right)}{\frac{1}{4}(p_1 + 2p_2 + 3p_3 + 4p_4)}\right) \tag{8a}$$

and

$$c_{Si} = \min\left(1, \frac{N_F/Si_F}{2p_0 + \frac{3}{2}p_1 + p_2 + \frac{1}{2}p_3}\right) \tag{8b}$$

all instances of a in Equation 6 are replaced by c. In all three of these cases, we make the assumption that no Si−NH−Al groups form (i.e., substitution near aluminum but *not* at an acid site).

For comparison to elemental analysis information, the percent (w/w) nitrogen in the material can be estimated in terms of the Si/Al ratio, r, and the substitution ratio, ζ, according to

(58) Vega, A. J. *J. Phys. Chem.* **1996**, *100*, 833–836.

$$\%N(r,\zeta) \approx \frac{2\zeta M_N}{\frac{r}{1+r}M_{Si} + \frac{1}{1+r}M_{Al} + 2\zeta M_N + 2(1-\zeta)M_O + \left(\frac{1}{1+r} + 2\zeta\right)M_H} \times 100\% \quad (9)$$

where M_i denotes the molecular weight of element i. For NaY zeolites, replace the term $M_H/(1 + r)$ with $M_{Na}/(1 + r)$.

4. Results and Discussion

4.1. X-Ray Diffraction Analysis. The powder XRD patterns of the zeolites nitrided at different temperatures for different times are shown in Figure 2. The nitrided HY (Si/Al = 15), NaY (Si/Al = 2.55) and HY (Si/Al = 2.55) samples all maintain a faujasite (FAU) structure with only slight decreases in crystallinity, particularly for NaY heated at high temperatures. Noticeable decreases in the intensities of some of the reflections (e.g., 220 and 711) occur as the reaction proceeds, indicating that structural changes have occurred. In contrast, the NH_4Y (Si/Al = 2.55) sample shows a much more pronounced loss of crystallinity after ammonia treatment. NH_4Y reacts to form HY during the dehydration process, and HY is known to be unstable above 500 °C due to dehydroxylation of the Si−O(H)−Al linkages to form Lewis acid sites and extraframework species.[59,60] This process occurs at much lower temperatures in the presence of water or steam.[61] In contrast, NaY zeolites are stable at higher temperatures. Thus, the difference in the framework stabilities following nitridation is attributed to the greater concentration of Si−O(H)−Al linkages in the NH_4Y sample as compared to the HY (Si/Al = 15) sample, the rupture of these linkages due to the elevated temperature (and water released due to nitridation) presumably competing with the nitridation mechanism. The HY sample (Si/Al = 2.55) contains a significant concentration of extra-framework aluminum atoms (as discussed in section 4.3.2 below), resulting in a lower aluminum content for the framework (Si/Al ratio of 6.1, as reported in our previous paper). This is consistent with the enhanced stability of this zeolite.

4.2. Nitrogen Content and Porosity. The results of nitrogen adsorption (measurement of the micropore volume and BET surface area, Table 1) all indicate that no severe structural damage has occurred during the high temperature treatment for the nitrided HY (Si/Al = 15 and Si/Al = 2.55) and NaY samples. The two HY zeolites with high and low aluminum content maintain a higher microporosity than the other samples, losing only 25% of their porosity upon nitrogen treatment at all temperatures studied. In contrast, nitrided NaY and NH_4Y zeolites show a 50−80% decrease in their micropore volumes, the larger loss in pore volume correlating with the loss in framework crystallinity, as seen by XRD for NH_4Y (Figure 2).

Nitrogen content analyses by both elemental analysis and by EDX measurements demonstrate that high concentrations of nitrogen are present, more than 30% of the weight of the material being replaced by nitrogen in the HY zeolites at the highest temperature studied (850 °C; Table 1), based on the EDX results. However, there are noticeable inconsistencies between the results of the two methods, with the combustion results showing noticeably lower nitrogen contents than those derived from EDX. The EDX nitrogen contents were calculated from the changes in the ratios of the Si and O intensities of the K-edges of the treated and the untreated zeolites, as shown in Figure 3 for Nit-NH_4Y-2.55−850−48, the Si intensity providing a standard with which to compare between the different samples.

Unfortunately, we were unable to obtain a standard material containing a known Si:Al:O:N ratio to help in these analyses, introducing a source of error. A more significant cause of the lower numbers obtained from combustion analysis is that the combustion reaction may not go to completion. A second source of error is the possible adsorption of water in the zeolites before the analysis, which is difficult to prevent since the chemical analyses are performed by a third party (Galbraith Laboratories). Any water absorption, which can be quite large if the zeolites are fully hydrated, will lead to higher than expected oxygen content in the materials. To check the reliability of the elemental analysis, we analyzed the nitrogen content of four batches of the same Nit-NH_4Y-2.55−850−48 sample by both combustion and Kjeldahl methods. Four different combustion analysis runs of the same sample gave nitrogen content results in the 7 to 14 weight percent range, whereas the same number of Kjeldahl method analyses indicated 15 to 20 weight percent nitrogen, suggesting that neither method is reliable. In contrast, EDX indicated that there is approximately 31% by weight nitrogen (68.2 mol % nitrogen of the total anion (O + N) content) in this material. This is much closer to the nitrogen contents estimated based on the ^{29}Si NMR results (see below). We note that elemental analysis, and weight gain in a TGA experiment (which also relies on a combustion reaction), represent the standard methods for characterizing nitrogen content of these materials,[9] providing further motivation for our detailed ^{29}Si NMR analyses of these materials.

Interestingly, the EDX analyses of the NH_4Y samples reveal a small amount of sodium. This is probably due to the presence of residual sodium cations located at the SI position, due to incomplete ion-exchange.[62] Finally, it should be noted that all the nitrogen determination measurements measure the total nitrogen content in the materials, not only the framework nitrogen content.

4.3. Structural Characterization by NMR Spectroscopy.

4.3.1. Predicted Chemical Shifts. We desire several answers from the calculations: we wish to predict which resonances correspond to each silicon environment, provide an estimate of the degree of substitution, and estimate the relative reaction energies that result from substitutions in particular locations. The relevant reaction here is NH_3 + zeolite = H_2O + N-zeolite.

Results of the NMR calculations for the central silicon atom in each cluster are shown in Table 2 for the acid form and Table 3 for the sodium form. Numbers given as ranges indicate several calculations were done with hydrogen, sodium, nitrogen, and/or aluminum atoms in different locations (e.g., a substitution at position O^{II} instead of position O^{IV}). The energies shown in Tables 2 and 3 are changes in the electronic energy due to the reaction NH_3 + zeolite = H_2O + N-zeolite. Corrections for zero-point energy, thermal energy, and entropy can be included by doing a frequency calculation, but we find that these corrections are small for most environments (see Supporting Information). We have therefore omitted thermal corrections

(59) Kao, H. M.; Grey, C. P. *J. Phys. Chem.* **1996**, *100*, 5105–5117.
(60) Luz, Z.; Vega, A. J. *J. Phys. Chem.* **1987**, *91*, 374–382.
(61) Wouters, B. H.; Chen, T.; Grobet, P. J. *J. Phys. Chem. B* **2001**, *105*, 1135–1139.
(62) Ciraolo, M. F.; Hanson, J. C.; Grey, C. P. *Microporous Mesoporous Mater.* **2001**, *49*, 111–124.

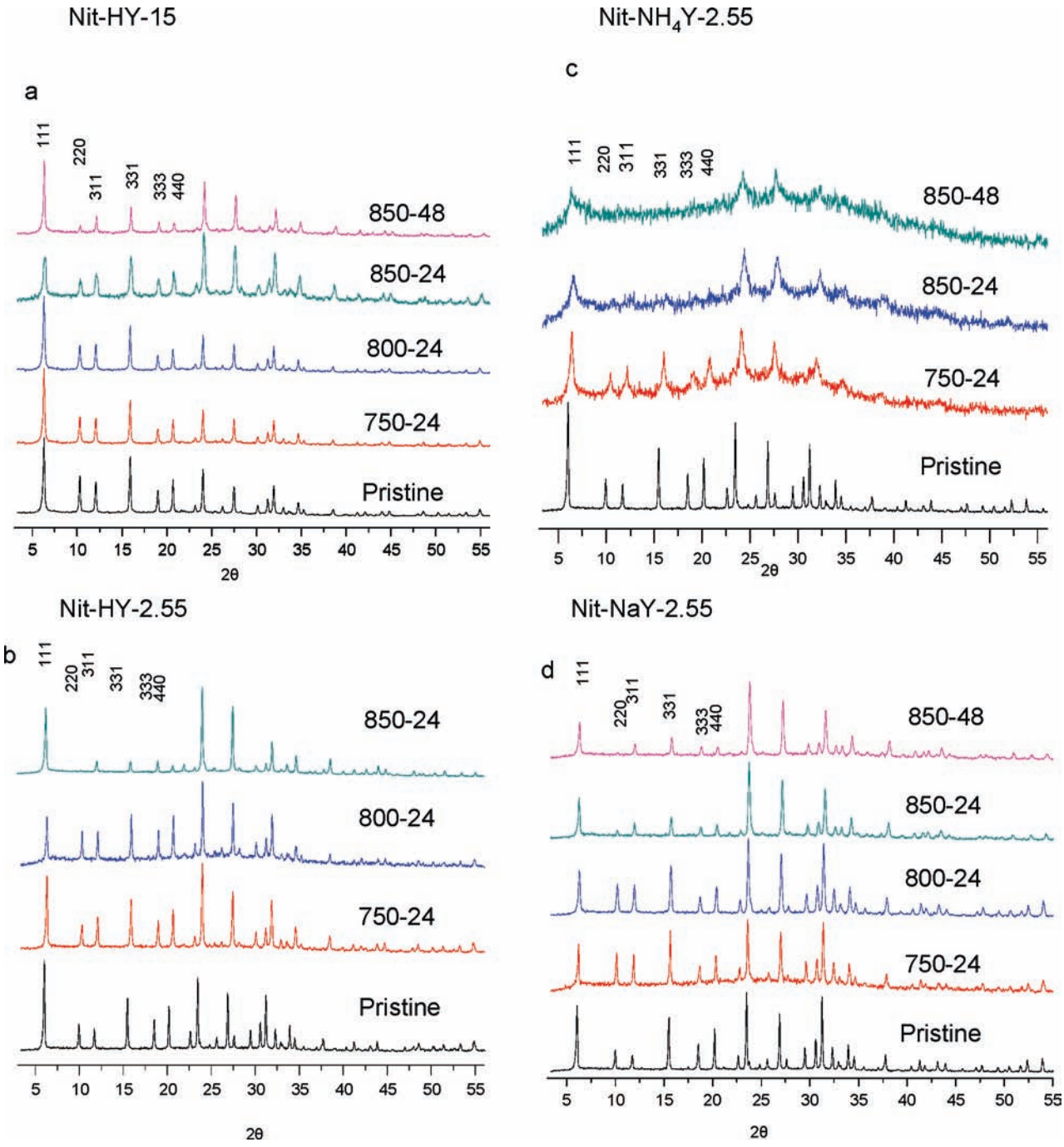

Figure 2. Powder XRD patterns for nitrided zeolite Y (Cu K-α). The first six reflections of the faujasite cell are indexed.

to the energy in the tables due to the extra resources required to do vibrational calculations on such a large cluster.

There are three trends in energy that are roughly additive. Substitution of the OH group of a Brønsted acid site with NH_2 is endoergic by about 35 kJ/mol, while substitution of oxygen with NH between two silicon atoms is endoergic about 100 kJ/mol. Substitution between silicon and aluminum but *not* at an acid site costs 120 kJ/mol or more. This suggests that substitution at acid sites should be preferred thermodynamically over substitution elsewhere. However, kinetic limitations are also likely under the conditions of the reaction, so we take this as a first hypothesis only. We will report kinetic pathways for nitrogen substitution in a forthcoming paper.

Several trends are evident in the silicon chemical shift. The chemical shift increases by 5−7 ppm as the number of nearby aluminum atoms increases. This is similar to the trend observed experimentally.[63,64] Substitution at a Brønsted acid (OH) site by an NH_2 group changes the chemical shift by 12−15 ppm toward TMS (e.g., environments 6 and 8 from Table 2). Substitution between two silicon atoms changes the chemical shift by 20−22 ppm, regardless of the presence of aluminum near one of the *other* oxygen atoms (e.g., environments 1 and

(63) Klinowski, J.; Ramdas, S.; Thomas, J. M.; Fyfe, C. A.; Hartman, J. S. *J. Chem. Soc., Faraday Trans. 2* **1982**, *78*, 1025–1050.
(64) Melchior, M. T.; Vaughan, D. E. W.; Jacobson, A. J. *J. Am. Chem. Soc.* **1982**, *104*, 4859–4864.

Table 1. Nitrogen Content and Surface Area Analysis for Nitrided Zeolites

	nitrogen content					adsorption		
		EDX[a]		^{29}Si NMR % N subs.[a]				
nitrided zeolite	elemental analysis % w/w[a]	% w/w	% mole	expt.	calc.[b]	BET surface area (m^2/g)	C_{BET}	micropore volume (cm^3/g)
Nit.HY.Si/Al = 15.750.24		12.8	27.3	9.7	6.5	634.6	−62.7	0.23
Nit.HY.Si/Al = 15.800.24		21.7	46.1	25.9	17	597.1	−65.2	0.21
Nit.HY.Si/Al = 15.850.24	11.8	26.1	54.9	45.2	35	658.4	−69.6	0.22
Nit.HY.Si/Al = 15.850.48	13.9	34.7	73.2	46.6		665.7	−75.5	0.21
HYSi/Al = 15 pure								
Si/Al = 42 (from ^{29}Si NMR)						857.6	−59.7	0.32
Nit.NaY.750.24		5.6	13.3	5.3	5	348.2	−45.2	0.17
Nit.NaY.800.24		7.2	16.7	6.8		348.7	−47.2	0.16
Nit.NaY.850.24	5.4	15.6	36.9	35	28	193.6	−54.7	0.08
Nit.NaY.850.48	9.2			42		331.9	−49.7	0.15
NaYSi/Al = 2.5 pure								
Si/Al = 2.65 (from ^{29}Si NMR)						655.7	−45.6	0.31
Nit.HY.Si/Al = 2.55.750.24		9.4	22.1	19	12	475.3	−47.8	0.22
Nit.HY.Si/Al = 2.55.800.24		10.5	25.0	19	9			
Nit.HY.Si/Al = 2.55.850.24	10.2	29.8	65.1	53	40	427.8	−51.2	
HY Si/Al = 2.55 pure								
Si/Al = 6.1 (from ^{29}Si NMR)						638.0	−47.5	0.29
Nit.NH_4Y.750.24	7.4	16.4	34.9			291.9	−80.8	0.08
Nit.NH_4Y.850.24		22.3	49.2			178.1	−252.6	0.03
Nit.NH_4Y.850.48	8.4−10.5	31.3	68.2			152.3	−198.4	0.02
NH_4Y Si/Al = 2.5 pure								
Si/Al = 4.2 (from ^{29}Si NMR)						1110.3	−64.5	0.40

[a] For the elemental and EDX analyses, we report the percent of nitrogen of the total weight of the sample (% w/w), for ease of comparison with data for comparable materials reported in the literature. To allow comparison with the ^{29}Si NMR data, the EDX data have also been converted into percent nitrogen substitution by moles (N/(O+N)), calculated by using the molecular formula of the anhydrous zeolite. [b] The % substitution of the zeolite framework, calculated from the NMR experiments, is compared with the results obtained by simulation, using the calculated shifts for different silicon local environments.

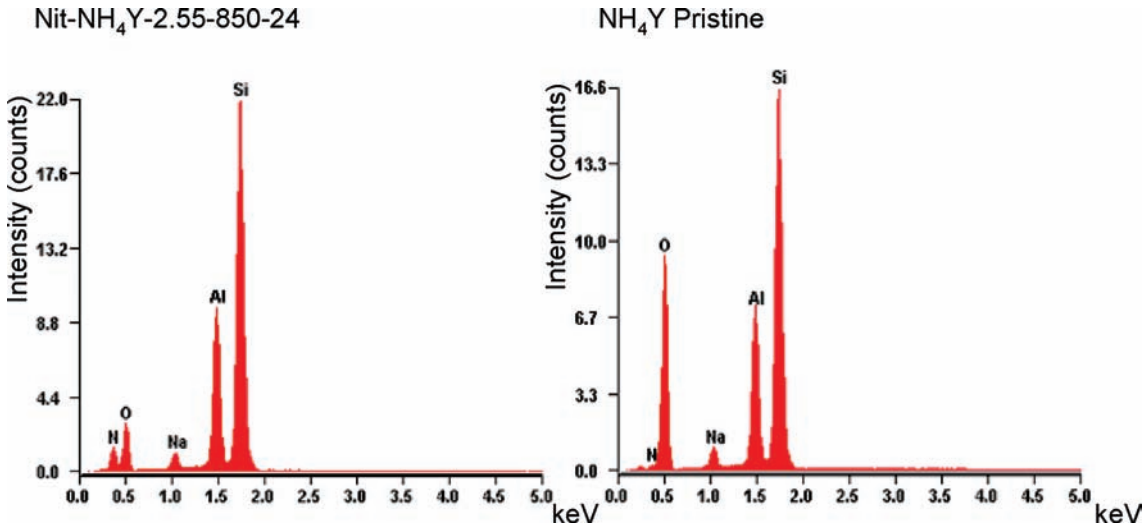

Figure 3. EDX analysis of ammonia treated and pristine zeolite NH_4Y.

2 or environments 6 and 10). It should be noted that the change in chemical shift gets smaller as the number of nitrogens added per silicon gets larger, presumably due to changes in Si−O−Si and Si−N−Si bond angles. Such strain effects are amplified by the finite cluster size and artificial termination.

Several chemical-shift ranges emerge for the different local environments:

−85 to −107 ppm unsubstituted
−71 to −89 ppm silicon near one nitrogen atom
−58 to −71 ppm silicon near two nitrogen atoms
−44 to −55 ppm silicon near three nitrogen atoms
−44 and higher silicon near four nitrogen atoms

The shifts for the different $SiO_{4-x}N_x$ local environments in silicon oxynitrides fall in these ranges (Table 2). Unfortunately, there are several local environments whose shifts lie outside these chemical shift ranges, especially those that contain larger numbers of aluminum atoms. For example, environment 27 (Table 2) has only one nitrogen substitution nearby, but its chemical shift is −67.1 ppm, putting it well into the category reserved for two nitrogen atoms when two or fewer aluminum atoms are involved. However, this and the similar structures that fall outside these ranges have three aluminum and three acid sites nearby the same Si. Energetically, it is most likely that one or two of the Bronsted-acid sites would bond to an O/N atom on the *other side* of the aluminum atom (i.e., not in the local coordination shell of the central Si). The range of chemical shifts given for environment 26 (−85.5 to −93.1 ppm) reflects the shift observed by moving *one* proton to the other

side of one of the aluminum atom, so in principle a similar shift will occur for environment 27 and others like it as well. If all these different environments are present, there is significant overlap in the chemical shift ranges, and no single region of the spectrum corresponds to a particular number of nitrogen atoms near one silicon atom. However, the high-aluminum

Table 2. Silicon Environments and the Corresponding Calculated Chemical Shifts for HY[a]

Structure	Environment	δ_{Si} (ppm)	ΔV (kJ/mol)	Structure	Environment	δ_{Si} (ppm)	ΔV (kJ/mol)
1	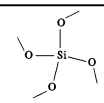	−107.4	-0-	17	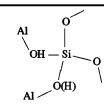	−92.3 to −94.3	-0-
2		−84.4 to −85.9	98.2–108.2	18	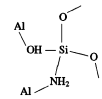	−81.4	35.7
3		−64.6	210.0	19	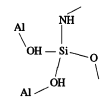	−71.0	103.9
4		−50.9	317.4	20	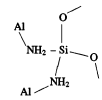	−67.1	70.5
5		−40.9	432.8	21	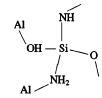	−61.3	149.7
6	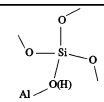	−99.5 to −101.3	-0-	22	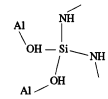	−44.8	200.1
7	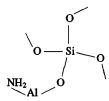	−99.8	41.4	23	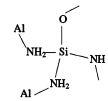	−44.7	180.0
8	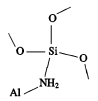	−86.5 to −88.1	32.3–55.2	24	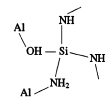	−37.3	249.5
9	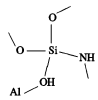	−78.1 to −81.3	92–105	25	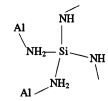	−32.5	296.0
10	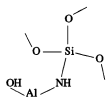	−76.8 to −79.0	121–127	26	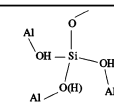	−85.5 to −93.1	-0-
11	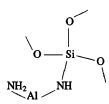	−75.7	171.3	27	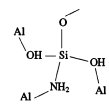	−67.1	34.8
12	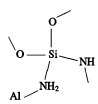	−67.7	140.5	28	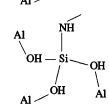	−65.3	96.3
13	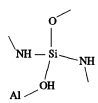	−63.1	221.7	29	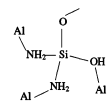	−51.6	65.1
14	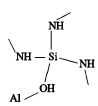	−51.4	341.0	30	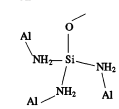	−45.5	104.0
15	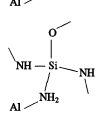	−47.8	249.1	31	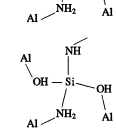	−39.7	141.7
16	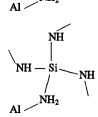	−37.5	368.7	32	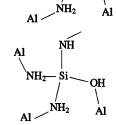	−28.5	176.9

Table 2. Continued

Structure	Environment	δ_{Si} (ppm)	ΔV (kJ/mol)
33	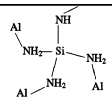	−24.4	224.1
34	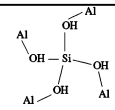	−76.7 to −82.1	-0-
35	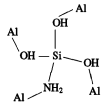	−54.4	28.1
36	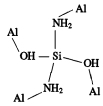	−37.7	79.8
37	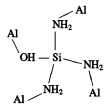	−23.5	114.5
38	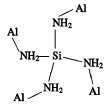	−10.3	132.6
Sites on a "surface" (terminal Si–OH, etc.)			
39	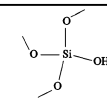	−94.6	-0-
40	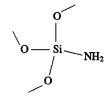	−78.7	30.1
Sites on an "edge" (terminal $Si(OH)_2$, etc.)			
41	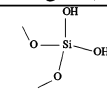	−80.4	-0-
42	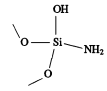	−67.3	52.0
43	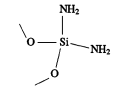	−62.0	104.8

[a] Atoms not drawn are implicitly part of a siliceous framework (SiO_2). Energies (ΔV) are electronic energies of reaction in the scheme NH_3 + zeolite = H_2O + N-zeolite.

environments occur with very low intensity in frameworks with low aluminum contents, so these categories can be used in such cases to provide an estimate of the degree of framework substitution based on experimental spectra.

One trend in the NMR calculations deserves special mention. The trend as the number of nearby aluminum atoms increases is to move the chemical shift to less negative values. Similarly, the trend in chemical shift as the number of nearby nitrogen atoms increases is to push the chemical shift to less negative values. One might then expect that environment 2 [Si(NH-Si)$(OSi)_3$] should have a more negative chemical shift than environment 8 [$Si(NH_2Al)(OSi)_3$], since it contains both an aluminum *and* a nitrogen atom. As can be seen from Table 2, however, the acid site substitution has the more negative chemical shift. This somewhat counterintuitive result is likely due to the fact that the substitution changes not only the atoms bound to the silicon but the bond angles around it as well.

We ran a series of calculations on silicic acid, $[Si(OH)_3]_2O$, and variants on it to test the sensitivity of the chemical shift to bond angle (Table 4). The immediate effect of a nitrogen substitution is to make the Si−X−Si or Si−X−Al bond more acute, making the chemical shift more positive. Substitution of nitrogen for oxygen also tends to make the chemical shift more positive, but structural constraints force the bond angle in the zeolite to be more obtuse than it would be in a free molecule, partially offsetting the atom effect. This effect could be responsible for the observation that $\delta_{Si\text{-}NH\text{-}Si} > \delta_{Si\text{-}NH_2\text{-}Al}$. That said, the observed difference is within the level of accuracy of the calculations and should be interpreted in that context.

We have included the computed chemical shifts of other nuclei (^{27}Al, $^{14,15}N$, $^{1,2}H$), as well as the predicted silicon chemical shifts of several extra-framework aluminum species inspired by the work of Mota,[65] in the Supporting Information.

4.3.2. ^{29}Si MAS NMR. Starting Materials. The spectrum of the HY zeolite with a nominal Si/Al elemental ratio of 2.55 is dominated by the $Si(OSi)_4$ and $Si(OAl)(OSi)_3$ resonances at −107 and −102 ppm, respectively. A noticeably higher Si/Al ratio of 6.1 for the zeolite framework than implied based on the Si/Al elemental ratio was extracted from the intensities of the different $Si(OAl)_x(OSi)_{4-x}$ resonances with Equation 1, indicating that significant dealumination has occurred. A similar phenomenon is observed for zeolite HY with a Si/Al elemental ratio of 15. Its spectrum is dominated by the $Si(OSi)_4$ resonance at around −107 ppm, yielding a Si/Al ratio of 42 for the framework. ^{27}Al MAS NMR of these samples (data not shown) contains signals at approximately 6 and 30 ppm, due to extra-framework 6- and 5-coordinate aluminum species, respectively. The significant concentration of extra-framework aluminum atoms is ascribed to a combination of the instability of the HY framework in the presence of moisture and the method used to prepare the lower aluminum content zeolites.[66,67] The ^{29}Si MAS NMR spectra of NaY and NH_4Y (Si/Al ratio = 2.55) are dominated by resonances at around −102 and −95 ppm, which are assigned to $Si(OAl)(OSi)_3$ and $Si(OAl)_2(OSi)_2$ sites, respectively (Figure 4). Analysis of the ^{29}Si NMR spectra of these materials indicates that the dealumination is minimal, and a Si/Al ratio of 2.65 is obtained. The Si/Al ratios of the framework of the four zeolites used in this study are summarized in Table 1.

Nit. HY (Si/Al = 15). Nitrided low-aluminum HY shows considerable nitrogen substitution following ammonia flow at high temperatures (Figure 4a). Slightly sharper line widths of the ^{29}Si resonances, as compared to the spectra of the other nitrided Y zeolites, are seen. This is attributed to the presence of fewer local silicon environments containing aluminum in the first coordination shells, and thus a smaller range of local

(65) Bhering, D. L.; Ramirez-Solis, A.; Mota, C. J. A. *J. Phys. Chem. B* **2003**, *107*, 4342–4347.
(66) Kerr, G. T. *J. Catal.* **1969**, *15*, 200–204.
(67) Wouters, B. H.; Chen, T.; Grobet, P. J. *J. Phys. Chem. B* **2001**, *105*, 1135–1139.

Table 3. Silicon Environments and the Corresponding Calculated Chemical Shifts for NaY[a]

Label	Environment	δ_{Si} (ppm)	ΔV (kJ/mol)	Label	Environment	δ_{Si} (ppm)	ΔV (kJ/mol)
44	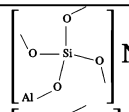 Na	−97.2 to −101.2	-0-	58	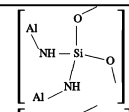 Na_2	−45.1	279.7
45	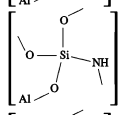 Na	−79.8	116.3	59	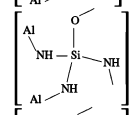 Na_2	−33.8	401.5
46	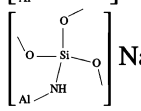 Na	−71.8 to −76.0	119.5–136.9	60	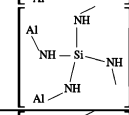 Na_2	−29.5	519.0
47	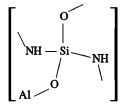 Na	−66.1	228.6	61	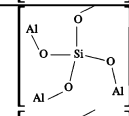 Na_3	−85.3 to −86.1	-0-
48	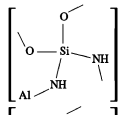 Na	−57.4 to −58.8	246.4–249.8	62	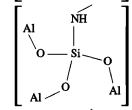 Na_3	−72.1	102.3
49	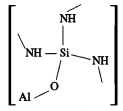 Na	−50.6	338.8	63	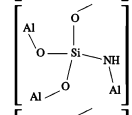 Na_3	−69.1	111.6
50	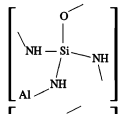 Na	−47.0 to −48.2	357.0–358.3	64	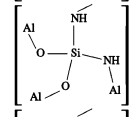 Na_3	−55.9	236.3
51	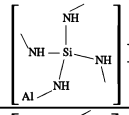 Na	−37.4	487.0	65	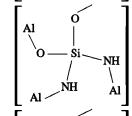 Na_3	−44.6	269.9
52	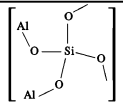 Na_2	−94.0 to −97.1	-0-	66	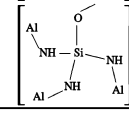 Na_3	−32.7	403.5
53	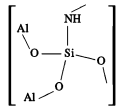 Na_2	−78.5	112.6	67	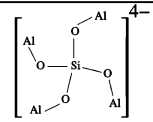	−79.8	-0-
54	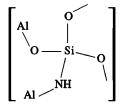 Na_2	−70.5	134.4	68	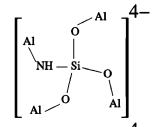	−63.5	151.9
55	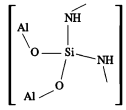 Na_2	−66.7	248.4	69	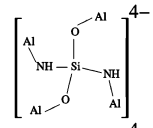	−48.9	296.7
56	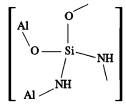 Na_2	−54.0	262.4	70	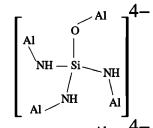	−37.9	458.0
57	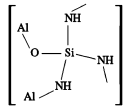 Na_2	−47.0	383.6	71	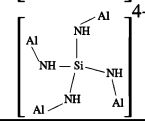	−28.7	589.1

[a] Energies (ΔV) are electronic energies of reaction in the scheme NH_3 + zeolite = H_2O + N-zeolite.

environments. As seen in Figure 4a, a new, asymmetric ^{29}Si resonance at approximately −86 ppm is observed along with a very weak resonance at around −66 ppm following ammonia treatment at 750 °C. The resonance at −102 ppm due to the $Si(OHAl)(OSi)_3$ environment (env. 6 in Table 2) has almost completely disappeared, indicating that these new resonances are due to nitrided silicon environments near both 0 and 1 aluminum atoms. On the basis of published literature[19] and the DFT calculations presented in Table 2, the −86 and −66 ppm peaks are assigned to $Si(NHSi)(OSi)_3/Si(NH_2Al)(OSi)_3$ (1N) and $Si(NHSi)_2(OSi)_2/Si(NH_2Al)(NHSi)(OSi)_2$ (2N) resonances, respectively. The loss of the $Si(OHAl)(OSi)_3$ resonance suggests

Table 4. Effect of Bond Angle on the Chemical Shift of Silicic Acid, $[Si(OH)_3]_2O$[a]

Molecule	Bond angle degrees	δ_{Si} (ppm)
$(OH)_3SiOSi(OH)_3$	138.3	−70.3
	147.6	−72.3
$(OH)_3SiNHSi(OH)_3$	129.6	−53.2
	135.9	−53.8
$(OH)_3SiOHAl(OH)_3$	130.1	−65.4
	134.2	−65.3
$(OH)_3SiNH_2Al(OH)_3$	110.7	−55.2
	125.6	−53.9

[a] The first angle listed for each compound is the equilibrium bond angle for the molecule. The second angle is the bond angle for one of the sites within the FAU framework.

that there is some preferential substitution of terminal silanol groups and Si−OH−Al linkages, which is consistent with the lower energies associated with these reactions as explained in section 4.3.1. This is explored in more detail in the next section.

Upon increasing the temperature to 800 °C, the intensity of the 1N (−86 ppm) resonance has increased and the −66 ppm (2N) resonance becomes more pronounced. A new peak at around −53 ppm, assigned to silicon near three NH/NH_2 groups (3N), is also observed. The −108 ppm $Si(OSi)_4$ resonance decreases in intensity, broadens, and shifts to −105 ppm. This shift and broadening is ascribed to distortion of the bond angles and bond lengths of the $Si(OSi)_4$ groups due to the nitridation of nearby sites (and/or the formation of defects). Upon reaching the maximum treatment temperature of 850 °C, a broad shoulder appears at around −43 ppm, the intensity of the high frequency peaks growing with reaction time. Given the almost complete disappearance of the 0N resonances in Nit-HY-15−850−48, where the spectrum of the starting material is dominated by this resonance, the 1−4N resonances in this sample material are likely dominated by environments that do not contain any aluminum in their local coordination shells. Thus, we assign the resonances at −86, −66, −53, and −43 ppm to $Si(NHSi)_x(OSi)_{4-x}$, with $x = 1$, 2, 3, and 4, respectively. Close examination of the resonances reveals that weaker resonances are hidden under the dominant resonances, which are assigned to environments containing aluminum and possibly NH_2 groups. In particular, the 1N resonance in the Nit-HY-15−750−24 spectrum shows noticeable asymmetry, which we ascribe to different local environments such as $Si(NHSi)(OSi)_3$ and $Si(NH_2Al)(OSi)_3$, which based on our DFT calculations (Table 2) result in less negative chemical shifts than the OAl environment.

Proton-^{29}Si CP MAS NMR spectroscopy was performed to investigate the proximity of the hydrogen and silicon atoms. The CP enhancements, obtained by comparing the intensities of the resonances obtained in the CP spectra acquired at short contact times (ct = 0.1, 0.2, and 0.5 ms) with those seen in the single pulse experiments, are −66 ppm (2N) > −86 ppm (1N) ≫ −107 ppm for Nit-HY-15−800−24 (Figure 5a). CP enhancements, particularly at short contact times, reflect silicon environments near a larger number of protons, since the larger the number of protons in the group, the stronger the ^{29}Si−^{1}H dipolar interaction and the faster the transfer of magnetization from the ^{1}H to ^{29}Si nuclei. This is consistent with the argument that the higher frequency resonances are due to silicon near increasingly larger numbers of nitrogen, since the substituted nitrogen will be present in the form of an NH group (or NH_2 for Si-NH_2−Al linkages), confirming our spectral assignments. ^{1}H/^{29}Si CP MAS NMR experiments on the other nitrided HY-15 nitrided samples are in agreement with this conclusion. Although a peak at around −43 ppm has been assigned as Si_2NH and $Si(NH)_2$ by other authors,[19] we assign this broad shoulder on the basis on the CP results, and the calculations presented in Table 2, to a combination of $Si(NHSi)_4$ sites and possibly terminal sites that contain four nearby nitrogen atoms.

Given the different errors associated with the various elemental analysis methods, we require a more reproducible and reliable method for establishing framework nitridation level. To this end, the percent nitrogen substitution was calculated from the single pulse ^{29}Si MAS NMR spectra (Table 1) by determining the intensity of each $Si(NH_yT)_x(OSi)_{4-x}$ resonance by spectral deconvolution as follows. We assume that the resonances centered at −107, −86, −66, −53, and −43 ppm correspond to $x = 0$, 1, 2, 3, and 4 nitrogen substitutions near one silicon atom, respectively, and that any overlap between spectral regions of the $Si(NH_yT)_x(OSi)_{4-x}$ resonances is accounted for in the peak deconvolution. The relative numbers of framework nitrogen and oxygen atoms are obtained by multiplying the intensity of each resonance by x and $4 - x$, respectively. This calculation implicitly assumes that nitridation of Si−O−Al, Si−O(H)−Al, and Si−O−Si bonds occurs randomly, the need for this assumption arising from the fact that we do not see the T sites occupied by aluminum. This assumption will be tested via our simulations of the spectra based on the chemical shift calculations. Note that a preference for Si−O(H)−Al or Si−O−Al substitution will result in an underestimation of the nitrogen content of the framework with this method, since the number of substitution sites per silicon atom is higher when aluminum atoms are present. The numbers based on NMR are intermediate between those estimated based on nitrogen elemental analysis and EDX. However, nitrogen contents based on the NMR spectrum reflect the nitrogen content of the *framework*, and the higher nitrogen content seen by EDX may reflect a higher nitridation level of the extraframework aluminum species. This will probably be more significant for samples nitrided at lower temperatures, since they should, kinetically, be easier to nitride than the framework. This method will also underestimate the nitrogen content if there are significant numbers of terminal Si-NH_2 groups (environment 40 in Table 2), which may also account for some of the differences between the two methods, particularly at the highest temperature.

Nit.HY with Si/Al = 2.55. Upon nitridation at 750 °C (Figure 4b), the ^{29}Si MAS NMR spectrum of HY contains two new resonances at around −83 ppm (1N) and −66 ppm (2N), which are noticeably broader than the 1N and 2N resonances seen in the lower aluminum HY sample. The $Si(OHAl)(OSi)_3$ site (−102 ppm) has almost completely disappeared, indicating that (a) preferential attack of the Si−O(H)−Al sites has occurred, and (b) that many of the new silicon sites must contain aluminum atoms in the first cation coordination shell, accounting for the additional broadening of these resonances. Distinct resonances are observed in the ^{29}Si NMR of Nit-HY-2.55−800−24, the chemical shift ranges due to 1N and 2N containing at least two different resonances at −86 and −81 ppm (1N) and −68 and −63 ppm (2N). Since substitution of aluminum for silicon in the SiO_2 framework causes a shift of approximately 5 ppm per aluminum atom, and lower frequency resonances (−86 and −68 ppm) are the dominant resonances in low aluminum HY zeolite, it is possible that the high frequency resonances arise from silicon near aluminum atoms,

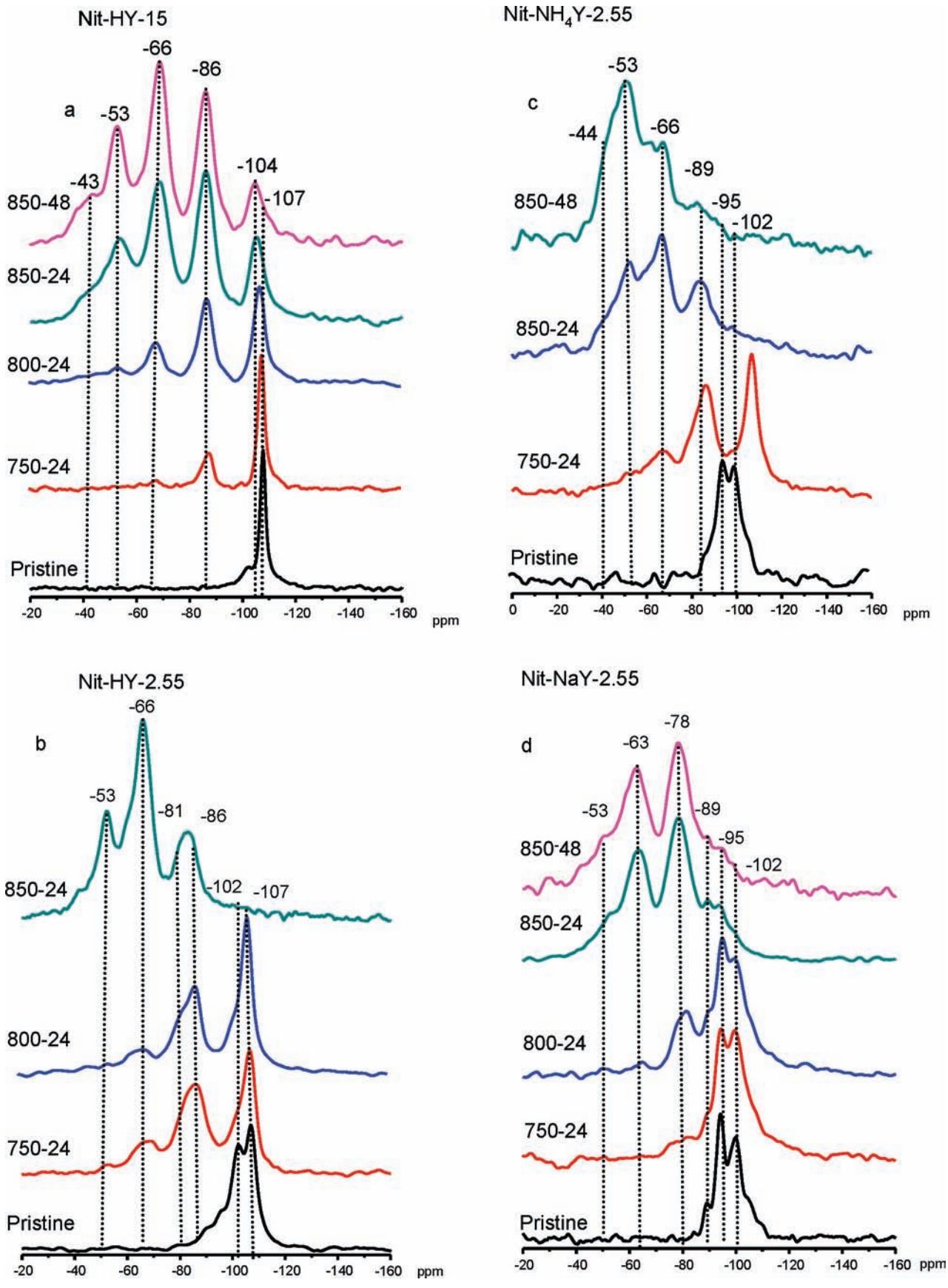

Figure 4. ^{29}Si SP MAS NMR of nitrided zeolite Y.

e.g., environments such as Si(OAl)(NHSi)$(OSi)_2$. However, since the bond angles of the Si−N−Al linkages are strained due to the rest of the zeolite framework, and the calculations (Table 2) indicate that Si-NH_2−Al environments resonate at a

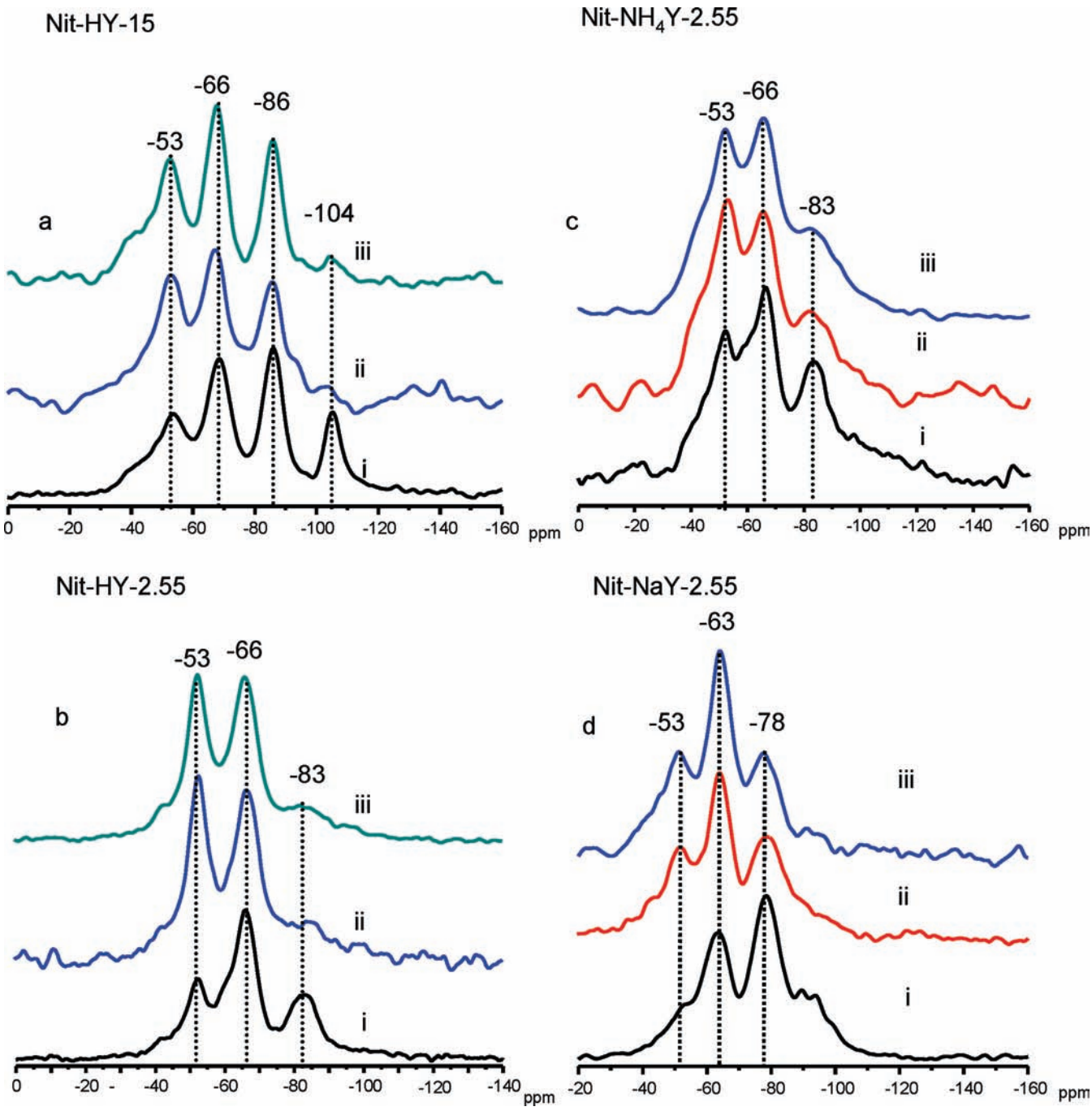

Figure 5. ^{29}Si SP (i) and CP MAS NMR (ii and iii, contact times of 0.2 and 0.5 ms, respectively) comparison of nitrided zeolite Y. Samples are prepared under ammonia at 850 °C for 24 h.

lower frequency than Si−NH−Si bonds, the assignment of the higher frequency shoulder remains ambiguous. Terminal sites such as $Si(OSi)_3NH_2$ or terminal sites with even higher nitrogen contents may also be present, producing even further peak broadening. The nitrogen substitution levels calculated by NMR (Table 1), as for the lower aluminum content material, fall in between those estimated based on nitrogen elemental analysis and based on EDX.

Upon increasing the reaction temperature to 850 °C, almost no sign of the $Si(OSi)_3$ and $Si(OHAl)(OSi)_3$ resonances from the pristine material are seen, and the spectrum is dominated by the 2N resonance at −66 ppm. The weak shoulder around −44 ppm is assigned to the 4N environments $Si(NHSi)_4$, $Si(NH_2Al)(NHSi)_2(OSi)$, and $Si(NH_2Al)_2(NHSi)(OSi)$. As can be seen in Table 2, surface substitutions (envs 40, 42, and 43) cannot account for this peak. Essentially all of the tetrahedral sites are substituted by at least one nitrogen atom without significant change in the crystal structure of the zeolite (Figure 2). This is consistent with the EDX elemental analysis, which indicates that 65.1% of the oxygen atoms have been replaced by nitrogen atoms (Table 1). Sharper resonances, particularly for the 2N and 3N environments, are seen at higher temperatures. This is probably because at higher reaction temperatures, all Brønsted acid sites have been substituted and only Si−O−Si linkages (and nonprotonated Si−O−Al linkages) remain. Any further reaction therefore does not create such a large variety of sites. For example, the Nit-HY-2.55−800−24 sample is dominated by the

$Si(OSi)_4$ resonance, which on nitridation at 850 °C, (where this signal has completely disappeared) will only produce $Si(OSi)_{4-x}(NHSi)_x$ resonances. $^1H/^{29}Si$ CP MAS NMR results are also consistent with these assignments (Figure 5b). The −66 ppm and −52 ppm resonances have enhanced peak intensities even at short contact times (0.1 to 0.5 ms), confirming that these sites are near more protons.

Nit.NH_4Y with Si/Al ratio = 2.55. The spectrum of NH_4Y zeolite following treatment at 750 °C (Figure 4c) is similar to that of HY with an Si/Al ratio of 2.55, and the resonances can be similarly assigned. What is significant, however, is the dramatic decrease in the intensity of the resonances due to the $Si(OHAl)(OSi)_3$ and $Si(OHAl)_2(OSi)_2$ sites in the ^{29}Si MAS NMR, the resonance due to the residual $Si(OSi)_4$ sites dominating the spectrum. This appears to suggest a strong preference for nitridation of the environments containing aluminum. In this higher aluminum content zeolite, the nitridation is accompanied by a significant loss of crystallinity, as seen by XRD (Figure 2) and via the loss in micropore volume (Table 1). This dealumination will generate terminal defects in form of silanols, which should be easily nitrided. The loss of crystallinity and the variety of different nitrided species most likely contribute to the very broad resonances seen in this system, which are particularly pronounced following nitridation at 850 °C for 24 and 48 h. The $^1H/^{29}Si$ CP MAS NMR data of nitrided NH_4Y also indicate that the environments corresponding to −52 and −43 ppm are highly protonated (Figure 5c). Given the breadth of these spectra, we did not attempt to deconvolute the line shapes and use the ^{29}Si NMR spectra to extract the nitrogen content.

Nit.NaY with Si/Al ratio = 2.55. Although the NaY zeolite used herein has the same Si/Al ratio as the NH_4Y zeolite, NaY shows the least nitrogen substitution of all the zeolites treated with ammonia at high temperatures (Figure 4d). Only negligible substitution is seen at 750 °C, and only the formation of a weak resonance at around −80 ppm is observed. This is consistent with the energy calculations, since the substitution between silicon and aluminum but *not* at an acid site costs more than 120 kJ/mol (compared to 100 kJ/mol for substitution at a Si−O−Si site). The sample prepared at 800 °C for 24 h is still dominated by the 0N (SiO_4) resonances of the pristine zeolite, but now the new (1N) resonance at −81 ppm, with a shoulder around −78 ppm, is clearly resolved. The chemical shifts of these 1N resonances are less negative than the 1N resonances in the HY samples with lower aluminum content, which is ascribed to the presence of more aluminum atoms in the local silicon coordination shell. Some differences between the chemical shifts will also arise due to the replacement of H^+ by Na^+; this is also observed in the calculated shifts (Tables 2 and 3). For example, the 1N silicon resonance for H^+ zeolite shows a chemical shift within the range of −88 to −81 ppm, whereas the same site for Na^+ zeolite has a shift of approximately −78 ppm.

On increasing the temperature to 850 °C, new sites with resonances at −63 and −53 ppm are observed, but the reaction does not go to completion. Even the spectrum of the material prepared at 850 °C for 48 h still contains the −95 ppm ($Si(OAl)_3(OSi)$) resonance from the pristine NaY zeolite. The intensities (relative to those in the untreated material) of non-nitrogen substituted sites are $Si(OAl)_3(OSi) > Si(OAl)_2(OSi)_2 > Si(OAl)(OSi)_3$. This suggests that nitridation is slightly biased toward Si−O−Si sites for zeolite NaY. This phenomenon appears to occur at all temperatures studied, a comparison of the relative intensities of the ^{29}Si resonances of nitrided NaY zeolite prepared at 750 and 800 °C also suggesting that nitrogen substitution occurs preferentially at silicon oxide tetrahedra with lower numbers of nearby aluminum atoms. This is supported by the higher energy of Si−NH−Al substitutions relative to Si−NH−Si substitutions. $^1H/^{29}Si$ CP NMR (Figure 5d) and CP kinetics for each resonance (not shown) show that the −53, −63, and −78 ppm sites are in closer proximity to more protons than the other sites, confirming that those resonances correspond to nitrogen substitution.

The nitrogen content values calculated by NMR are lower than those obtained by EDX analysis, as was the case for the other treated zeolites, for the materials treated at 750 and 800 °C. However, for the material treated at 850 °C, the NMR and EDX results are similar. We observe similar trends for the other high temperature treated zeolites. This may be related to the fact that EDX is more sensitive to the elemental composition closer to the surface than in the center of the particle (i.e., the first 0−0.75 mm), suggesting that the substitution at lower temperatures may be less uniform than the substitution at high temperatures. We note that the slight tendency for substitution at Si−O−Si vs Si−O−Al sites means that, in contrast to the HY samples, this NMR method will lead to a slight overestimation of the nitrogen content of the framework.

4.3.3. Simulating the NMR Spectra. The values of the chemical shifts from DFT calculations (section 4.3.1), combined with the experimental spectra (section 4.3.2), have given us a good indication of which peaks in the NMR spectra (Figure 4) correspond to which chemical environments (Tables 2 and 3). We now fit the intensities of each peak using the procedure outlined in section 3.2 to obtain information about the relative substitution level in the zeolite framework and explicitly explore the effect of preferential reaction at Si−O−Si vs Si−O(H)−Al sites. Our first task is to fit the spectrum of the untreated zeolite. For nitrided zeolites HY with Si/Al ratios of 2.55 and 15, this fit is shown in Figure 6.

Both of the HY zeolites exhibit considerable dealumination: the best-fit Si/Al ratio for HY with Si/Al = 2.55 is 6.1−6.3 (a value of 6.25 was used). Similarly, the material with Si/Al = 15 appears to have a frameowork Si/Al ratio of approximately 42. These values are consistent with the ratios calculated by NMR data in section 4.3.2 using eq 1. Our attempted fit of the spectrum in Figure 4b corresponding to a temperature of 750 °C using eq 6 and the various probabilities of eqs 5a, 7, and 8a is shown in Figure 7. The best fit is actually a sum of the spectra generated using probabilities *a* (attack of acid sites first) and *b* (unbiased substitution), weighed accordingly with a bias ratio (BR): $S(\delta) = \mathrm{BR}\ S(\delta|a) + (1 - \mathrm{BR})\ S(\delta|b)$, where $S(\delta|a)$ denotes the spectrum generated by assuming the probabilities *a* (eq 5a) in eq 6. Biasing the substitutions to aluminum or silicon sites alone fails to create the appropriate asymmetry in the peak in the −80 to −90 ppm region, and being completely unbiased fails to predict the disappearance of the peak corresponding to environment 6 (Table 2) near −100 ppm. The fitting parameter BR, for "bias ratio," reflects the fraction of the substitutions that are biased toward Brønsted acid sites (i.e., BR = 1 corresponds to the acid sites filling first, and BR = 0 indicates no bias).

The spectra of the other HY zeolites can be fitted with similar assumptions, as shown in Figure 8. Except as noted, the same

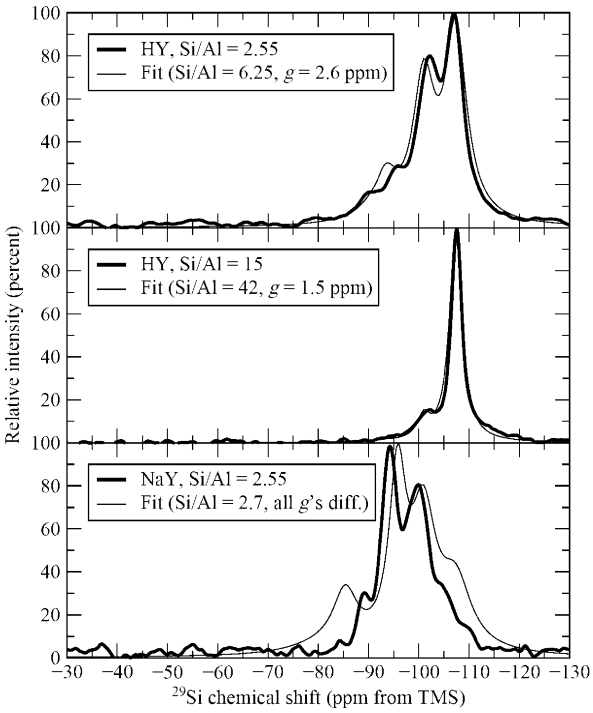

Figure 6. Fits to the untreated spectra of zeolite HY, Si/Al = 2.55 (top), HY, Si/Al = 15 (middle), and NaY, Si/Al = 2.55 (bottom) using chemical shifts from Tables 2 and 3 and intensities from Vega.[58] The fitted Si/Al ratios are 6.25 (top), 42 (middle), and 2.7 (bottom); the fitted line widths are 2.6 ppm (top), 1.5 ppm (middle), and several values (bottom; see text).

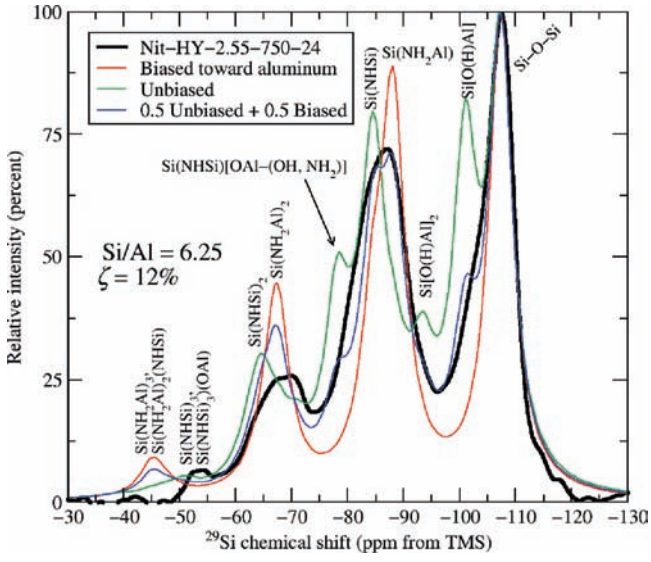

Figure 7. Fitted spectrum of HY zeolite (Si/Al = 2.55) treated for 24 h at 750 °C using eqs 5a ("Biased toward aluminum"), eq 7 ("Unbiased"), and the sum of the two with a bias ratio of 0.5 ("Summed").

value of g (the line-broadening parameter) was used to fit both the treated and untreated spectra for the same starting material. In only one case shown in Figure 8 (HY-15−850−24) was it necessary to change the line width g to get a significantly better fit, though there are some cases for which adjusting this parameter would help the fit. It should be noted that the bias ratio (BR) makes little or no difference in the quality of fit for the low aluminum materials (HY, Si/Al = 15) at high nitridation levels: changing whether acid sites react first or not makes little difference when there are relatively few acid sites.

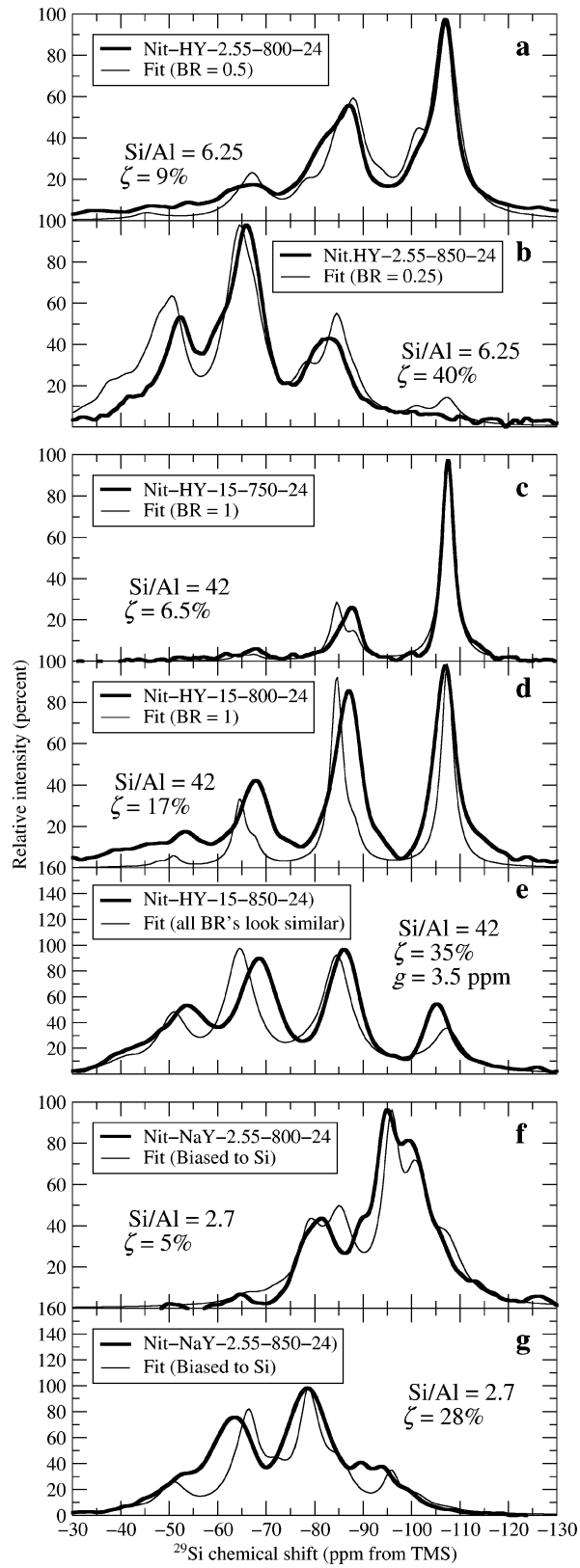

Figure 8. Fitted spectra of several materials and the fitting parameters (ζ) that best fit the spectra. The value of ζ (the fractional substitution [ζ = N/(N+O)]) is adjusted until the visual fit is best. Plots for HY are fitted via eqs 5a and 7; those for NaY use eqs 8a.

Fitting the NaY spectra, in general, is significantly more difficult than fitting the HY spectra. Part of this lies in the multiple locations that sodium ions can take. Commonly used nomenclature initiated by Pickert[68] labels these sites SI, SI′,

SII, SII′, SIII, and SIII′, meaning there are (at least) six different possible environments due to sodium cations. We did not simulate more than two environments for each structure, and in many cases in Table 3 we only chose cations at one set of positions (e.g., I, I, and III for a 3-Na environment). However, the fact that these sites play a role in the observed spectra is evident from the extra broadening associated with the SiO(1)Al peak in Figure 6. This extra broadening is usually handled by increasing the value of the line width g used to fit that particular peak in eq 3. We have done the same for NaY in Figure 6, where the associated widths of each peak are 3.7, 3.0, 2.0, 3.0, and 7.0 ppm for silicon atoms near 0, 1, 2, 3, and 4 aluminum atoms, respectively. How to transfer this broadening pattern to the substituted zeolites was not entirely clear, so we made the assumption that sites associated with a certain number of aluminum atoms nearby have the *same* width as the site with the corresponding number of aluminum atoms in the untreated spectrum. This produces the fits in Figure 8. Another reason fitting NaY spectra is more difficult is the more obvious presence of error in the calculations; this is most likely due effects like lattice distortion due to the presence of large numbers of aluminum atoms in the cluster (the terminal atoms of which are fixed at the same coordinates as they are in the siliceous framework). Consistent with this, the largest error in the shift occurs for the SiO(3)Al environment, because it contains the largest number of nearby Na^+ ions (of the environments that occur in significant concentrations) and will be associated with the largest local distortion, when compared with the average environment found in the siliceous framework. There may also be fundamental errors in the calculation method: For example, we assume that the constant of proportionality is unity between the calculated and experimental chemical shifts ($\delta = m\sigma + b$, $m = -1$); it has been suggested that this does not necessarily produce the best agreement with experiment.[69]

It is interesting to note the apparent trends in the preference of nitrogen to substitute between two silicon atoms versus between a silicon atom and an aluminum atom. In the case of low (<10%) substitution, there is a clear preference (BR $\approx$ 0.25−0.5) for substitution at *acid* sites. This is not surprising given the drastically lower energy of such substitutions. As the temperature is increased, however, the best fit bias ratio decreases, suggesting that the energy differences become less significant at high temperatures. In the case of NaY, where the energy of reaction is higher for reaction at Si−O−Al sites than Si−O−Si sites, substitution appears to be biased toward reaction between two silicon atoms.

It should be noted of course that *none* of the fits in Figures 7 and 8 is perfect, which is a reflection of errors in both the calculations and our fitting procedure (i.e., the assumption of random substitution). In general, the substitution pattern appears to deviate more from completely random behavior [i.e., eq 6] as the substitution ratio (ζ) increases. The peaks in the experimental spectra also tend to broaden, indicating the presence of angle strain and other small perturbations to the NMR signal. It should also be noted that ^{29}Si NMR spectroscopy alone cannot confirm whether nitrogen substitutes at Si−O−Si or Si−OH−Al sites, since there is some overlap between chemical shift ranges, particularly in the high-aluminum content materials. Aluminum-27 and ^{15}N MAS NMR data might provide a more complete picture of the nitridation mechanism; these studies are in progress. Finally, given the number of assumptions made in the extraction of the nitridation levels directly from the spectra, and the large amount of potential error and the various assumptions associated with the simulations, the agreement between the two methods is quite good (Table 1).

5. Summary and Concluding Remarks

The effects of aluminum content and charge-compensating cation on the nitridation of zeolite Y using high-temperature ammonia have been studied using a combination of modeling, NMR spectroscopy, adsorption, and X-ray diffraction. The appearance and evolution of new silicon resonances in the ^{29}Si MAS NMR spectra and the results of nitrogen content measurements of samples prepared at various temperatures using various reaction durations show that the degree of substitution increases with increasing reaction temperature and time. The effects of reaction conditions such as ammonia flow rate will be discussed in detail in a forthcoming publication. Zeolites with higher Si/Al ratios show more well-resolved and sharp ^{29}Si MAS NMR spectra and higher crystallinity after the reaction, whereas protonated acidic zeolites with high aluminum content lose their crystallinity and microporosity during the ammonia treatment. In particular, although nitrided NH_4Y undergoes the highest nitrogen substitution under the same conditions as compared to the sodium and low aluminum acidic zeolites, it decomposes in the process and therefore will be less useful as a catalyst for reactions that require high surface areas and shape selectivity arising from porosity. The presence of sodium as a charge-compensating cation provides higher stability, but decreases the extent of reaction.

The comparisons between measured and calculated ^{29}Si MAS NMR chemical shifts show good agreement, providing strong evidence that high levels of nitrogen substitution have been achieved. The calculations on small nitrogen-substituted zeolite clusters show that the nitridation reaction is energetically unfavorable, and that the expected energy of reaction for different silicon environments is Si−OH−Al < Si−O−Si < Si−O−Al. This is confirmed in the fits of the experimental spectra with the simulations for relatively low temperature treatments (Figure 8). This preference is less pronounced or absent for higher reaction temperatures, in part because all of the Si−O(H)−Al sites have already reacted at these temperatures. Nitrogen substitution of NaY zeolite shows a lower degree of substitution than the treated HY zeolites at low temperatures. This is supported by the calculations, which show a higher energy of substitution for the Si−NH−Al connectivity relative to the Si−NH−Si and Si−NH_2−Al connectivities. Sodium Y substitutions are slightly biased toward reaction of Si−O−Si over Si−O−Al groups, as seen in the analysis of the change in $Si(OSi)_{4-y}(OAl)_y$ resonances with temperature and in the simulations of the experimental data.

Adsorption isotherms show that the crystalline samples maintain substantial microporosity post-treatment, although some pore-blocking/loss of crystallinity has clearly occurred.

(68) Pickert, P. E.; Rabo, J. A.; Dempsey, E.; Schomaker, V. In *Zeolite Cations with Strong Electrostatic Fields as Carboniogenic Catalytic Centers*; Proceedings of the International Congress on Catalysis, 3rd, Amsterdam, 1964; North Holland: Amsterdam, 1965; pp 714−728.
(69) Baldridge, K. K.; Siegel, J. S. *J. Phys. Chem. A* **1999**, *103*, 4038–4042.

This shows that low-aluminum zeolites in particular can be treated with ammonia to produce crystalline, microporous, nitrogen-substituted zeolites. These materials are expected to behave as relatively strong solid base catalysts.[16] Future work is needed to investigate the detailed mechanisms of nitrogen substitution, as well as the applicability of these new materials as shape selective solid base catalysts.

Acknowledgment. F.D. and C.P.G. thank Baris Key at SBU for his assistance with building the experimental setup and for helpful discussions. F.D. also thanks Dr. James Quinn at SBU for his help in EDX experiments. K.H. thanks Dr. Justin Fermann at UMass for his expertise and Tim Landers at UMass for glassblowing services. This research was generously funded by the National Science Foundation (CBET-0553577) and the United States Department of Energy (DE-FG02-07ER15918 and DE-FG02-96ER14681).

Supporting Information Available: Table of zero-point energies, enthalpies, entropies, and Gibbs free energies of selected structures; chemical shifts and energies for substitutions of extraframework aluminum species; chemical shifts and quadrupolar coupling constants for ^{27}Al and $^{14/15}$N nuclei in the structure; and complete ref 47. This material is available free of charge via the Internet at http://pubs.acs.org.

JA9031133